



Assessment of fine and coarse tyre wear particles along a highway stormwater system and in receiving waters: Occurrence and transport

Downloaded from: <https://research.chalmers.se>, 2024-08-14 05:25 UTC

Citation for the original published paper (version of record):

Gaggini, E., Polukarova, M., Bondelind, M. et al (2024). Assessment of fine and coarse tyre wear particles along a highway stormwater system and in receiving waters: Occurrence and transport. *Journal of Environmental Management*, 367. <http://dx.doi.org/10.1016/j.jenvman.2024.121989>

N.B. When citing this work, cite the original published paper.



Research article

Assessment of fine and coarse tyre wear particles along a highway stormwater system and in receiving waters: Occurrence and transport

Elly Lucia Gaggini^{a,*}, Maria Polukarova^{a,b}, Mia Bondelind^a, Elisabeth Rødland^c, Ann-Margret Strömvall^a, Yvonne Andersson-Sköld^{b,d}, Ekaterina Sokolova^e

^a Water Environment Technology, Department of Architecture and Civil Engineering, Chalmers University of Technology, SE-412 96, Gothenburg, Sweden

^b Swedish National Road and Transport Research Institute (VTI), Box 8072, SE-402 78, Gothenburg, Sweden

^c Norwegian Institute for Water Research, Økernveien 94, NO-0579, Oslo, Norway

^d Division of Geology and Geotechnics, Department of Architecture and Civil Engineering, Chalmers University of Technology, SE-412 96, Gothenburg, Sweden

^e Uppsala University, Department of Earth Sciences, SE-752 36, Uppsala, Sweden

ARTICLE INFO

Handling Editor: Lixiao Zhang

Keywords:

Gully pot
Microplastics
Road runoff
Sampling
Tire
Tyre and road wear

ABSTRACT

Tyre wear has been identified as a major road-related pollutant source, with road runoff transporting tyre wear particles (TWP) to adjacent soil, watercourses, or further through stormwater systems. The aim of this study was to investigate the occurrence and transport of TWP along a stormwater system. Water and sediment have been sampled at selected points (road runoff, gully pots, wells, outlet to a ditch, and stream) through a stormwater system situated along a highway in Sweden during November and December 2022, and March 2023. As there is limited data on the size distribution of TWP in different environmental media, especially in the size fraction <20 µm, the samples were fractionated into a fine (1.6–20 µm) and a coarse (1.6–500 µm) size fraction. The samples were analysed using a combination of marker compounds (benzene, α-methylstyrene, ethylstyrene, and butadiene trimer) for styrene-butadiene rubbers with PYR-GC/MS from which TWP concentration was calculated. Suspended solids were analysed in the water samples, and organic content was analysed in the sediment samples. TWP was found at nearly all locations, with concentrations up to 17 mg/L in the water samples and up to 40 mg/g in the sediment samples. In the sediment samples, TWP in the size fraction 1.6–20 µm represented a significant proportion (20–60%). Correlations were found between TWP concentration and suspended solids in the water samples ($r = 0.87$) and organic content in the sediment samples ($r = 0.72$). The results presented in this study demonstrate that TWP can be transported to the surrounding environment through road runoff, with limited retention in the studied stormwater system.

1. Introduction

Recent studies emphasize the significance of tyre wear particles (TWP) as a major road-related pollutant source, and the occurrence of TWP has been reported in air, water, soil, sediment, and snow (Goßmann et al., 2023; Mengistu et al., 2021; Rauert et al., 2022; Rødland et al., 2023b; Vijayan et al., 2022). TWP represents a potential risk for aquatic organisms, especially due to the toxicity of leachates of zinc and organic compounds (Wik and Dave, 2009), and toxic effects have been confirmed (Tian et al., 2021). Estimates of tyre wear emissions in Sweden show that potentially large amounts spread to the environment

(Magnusson et al., 2016). Road runoff can be an important vector, transferring TWP directly to adjacent soil, or further through drainage systems (Wagner et al., 2018), but there is a large knowledge gap regarding the occurrence and fate of tyre wear once emitted to the environment (Andersson-Sköld et al., 2020).

TWP has been reported in stormwater and in sediments in stormwater systems (Järllskog et al., 2022a; Knight et al., 2020; Mengistu et al., 2021; Rødland et al., 2022a; Sutton et al., 2019), and rubber was identified as the most abundant type of microplastics in a stormwater system of a Swedish highway (Lange et al., 2021). However, analysis and monitoring of TWP in environmental samples are challenging

* Corresponding author. Department of Architecture and Civil Engineering, Chalmers University of Technology, SE-412 96, Gothenburg, Sweden.

E-mail addresses: elly.gaggini@chalmers.se (E.L. Gaggini), maria.polukarova@vti.se (M. Polukarova), mia.bondelind@chalmers.se (M. Bondelind), elisabeth.rodland@niva.no (E. Rødland), ann-margret.stromvall@chalmers.se (A.-M. Strömvall), yvonne.andersson-skold@vti.se (Y. Andersson-Sköld), ekaterina.sokolova@geou.uu.se (E. Sokolova).

<https://doi.org/10.1016/j.jenvman.2024.121989>

Received 15 May 2024; Received in revised form 20 July 2024; Accepted 23 July 2024

Available online 3 August 2024

0301-4797/© 2024 The Authors. Published by Elsevier Ltd. This is an open access article under the CC BY license (<http://creativecommons.org/licenses/by/4.0/>).

(Mattonai et al., 2022). Notably, many previous studies have not analysed the finer size fraction of TWP $<20\ \mu\text{m}$ (Järilskog et al., 2020; Knight et al., 2020; Lange et al., 2022; Vijayan et al., 2022). Thus, the amount of TWP in the samples may have been underestimated, as few other studies have highlighted that this size fraction constitutes a significant portion of the total TWP mass (Järilskog et al., 2022a; Klöckner et al., 2020). Moreover, the size distribution of TWP in both aqueous and sediment phases is important as it determines TWP fate in the environment.

Various analytical methods have been used to measure TWP in environmental samples, namely, light microscopy, Fourier-transform infrared spectroscopy (FTIR), scanning electron microscopy with energy dispersive X-ray spectroscopy (SEM-EDX), pyrolysis gas chromatography (PYR-GC/MS), and thermal extraction and desorption (TED-GC/MS). Light microscopy and FTIR have limitations in analysing finer particles $<10\ \mu\text{m}$ (Rødland et al., 2023a) and may be hindered by fillers such as carbon black (Eisentraut et al., 2018) or by mineral encrustations (Rødland et al., 2023a). SEM-EDX allows quantification of the number of particles, but also has limitations regarding identification of TWP $<20\ \mu\text{m}$ (Järilskog et al., 2022b). PYR-GC/MS and TED-GC/MS rely on the identification of different analytical marker compounds to detect specific tyre wear polymers for quantification (Mattonai et al., 2022) and do not have limitations related to particle size. However, for PYR-GC/MS and TED-GC/MS, the large variation in chemical composition among tyres poses challenges to assessing the tyre wear mass based on standardized marker levels (Rødland et al., 2023a). Given the analytical challenges with determining TWP concentrations, other environmental quality parameters that are easier to measure may be used to indicate the presence of TWP. For example, Total suspended solids has been suggested as an indicator for TWP content in road runoff (Vogelsang et al., 2019), and a strong correlation between Total suspended solids and TWP has been reported in tunnel wash water (Rødland et al., 2022a).

The aim of this study was to investigate the occurrence and transport of tyre wear particles in different matrices through a stormwater system at a Swedish highway and its receiving waters. The analysis was performed using PYR-GC/MS for styrene-butadiene rubber (SBR) and butadiene rubber (BR), coupled with Monte Carlo simulations to account for the variability in standardized markers in tyres. The objectives were to:

- Identify/estimate the TWP concentration in the water phase for the size fractions $1.6\text{--}20\ \mu\text{m}$ and $1.6\text{--}500\ \mu\text{m}$;
- Identify/estimate the TWP concentration in the sediment phase for the size fractions $1.6\text{--}20\ \mu\text{m}$ and $0\text{--}500\ \mu\text{m}$;
- Investigate the potential correlation between TWP concentration and Total suspended solids (TSS) and Volatile suspended solids (VSS) for the water phase, and Loss on ignition (LOI) for the sediment phase;
- Compare TWP concentrations at different locations within the stormwater system on different sampling occasions.

2. Material and methods

2.1. Study area

The sampling was performed along a part of highway E18 in Sweden, between the municipalities of Västerås and Enköping, at a site known as Testsite E18, Fig. 1. The test site is a road research facility owned by the Swedish Transportation Administration. The test site is marked in red in Fig. 1 ($59^{\circ}38'01.9''\text{N}$ $16^{\circ}51'18.7''\text{E}$). Testsite E18 is located in an open flat area surrounded mostly by agricultural land. The road section has about 10,000 AADT per highway direction, of which 1400 were heavy vehicles (Swedish Transport Administration, 2024). The highway has two lanes in each direction, and the speed limit is 120 km/h. The highway was built in 2010, and the current pavement type is stone mastic asphalt, and of the same type as the original cover. However, the current pavement also includes traces of polymer-modified bitumen, used for filling the wheel tracks in 2016, that was recycled into the current cover using warm-remixing in 2021.

For most parts of highway E18, the runoff from the road drains freely into the ditches at the sides of the road, but at Testsite E18 in the direction towards Enköping, a 100 m long kerbstone directs the runoff into two gully pots, locations G1 and G2 in Fig. 2A. The gully pots are serially connected, where gully pot (G1) drains into gully pot (G2). Gully pot G2 is thereafter connected to a well (location WA) equipped with a Thomson weir. The well WA drains into a final collecting well WF. The collecting well WF also receives stormwater from two additional wells WB and WC, which receive water infiltrated from the geo-textile lined ditches at the sides of the highway lanes in the direction of Enköping. The collecting well WF finally discharges runoff through a pipe into a ditch, which runs along the highway (location D). The ditch runs along the highway up until the bridge over the stream Lillån (location L). The

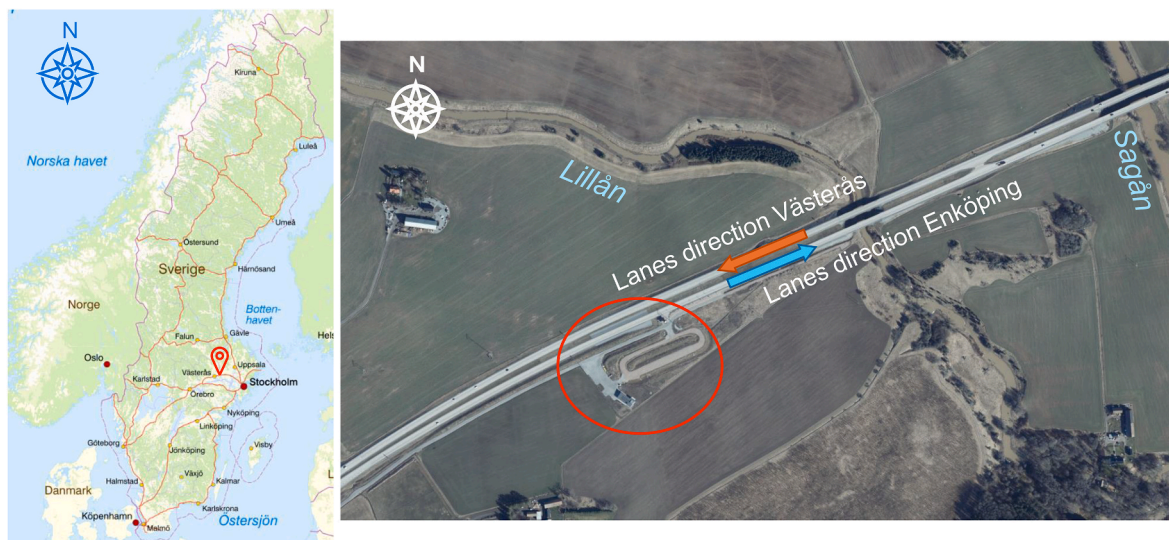


Fig. 1. Left: The location of the sampling site is shown by the red pin. Right: Map showing Testsite E18 marked with red circle, Sagån and Lillån streams marked with names, and the highway directions towards Västerås and Enköping marked with arrows. Maps collected and modified from Swedish Land Survey (2024). (For interpretation of the references to colour in this figure legend, the reader is referred to the Web version of this article.)

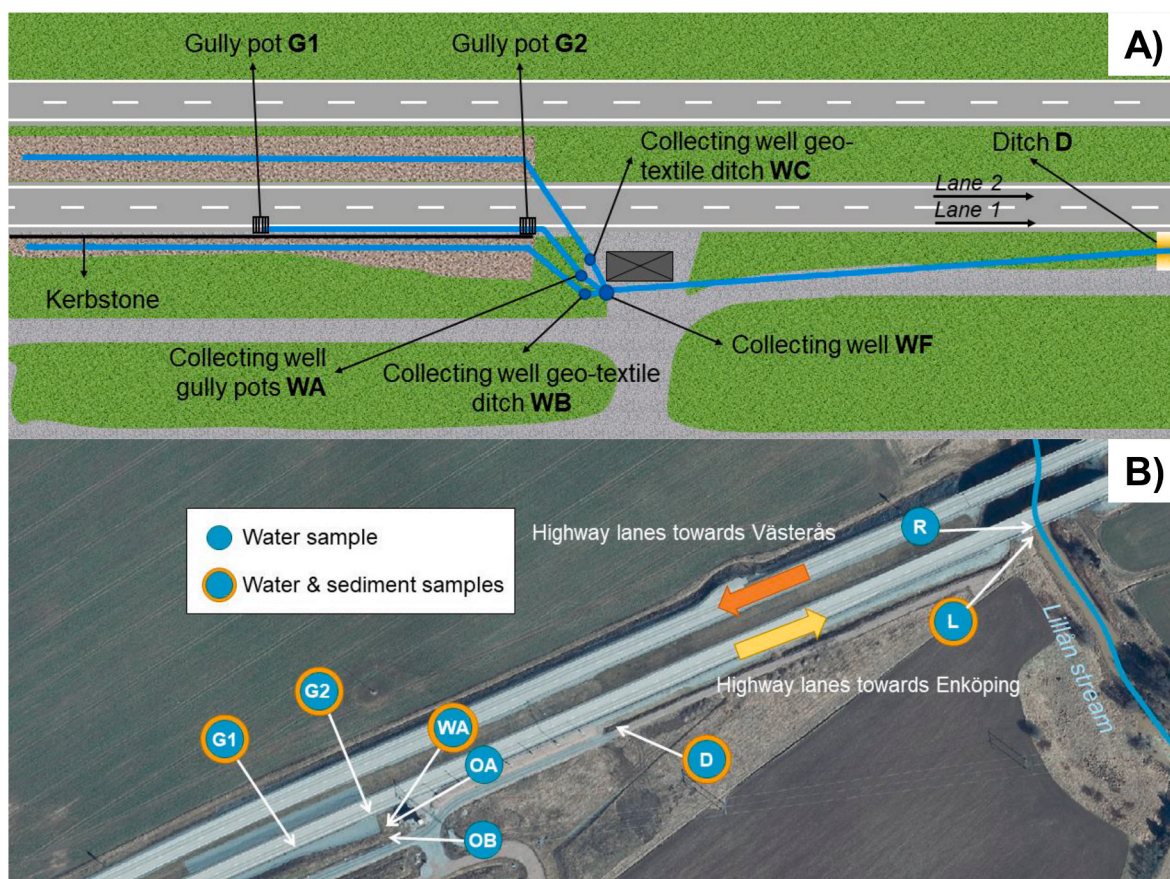


Fig. 2. A) Illustration of the stormwater system at Testsite E18. B) Map showing the sampling locations. Blue circles indicate grab samples of water; orange circles indicate grab samples of sediment. G1 is first gully pot, G2 is second gully pot, WA is standing water in weir volume of collecting well A, OA is outflowing water from weir in collecting well WA, OB is outflowing water from weir in collecting well (WB) gathering water from geo-textile ditch, D is outlet pipe in roadside ditch: sediment was collected within the outlet pipe and water from the standing water in the ditch that partially covered the outlet pipe, R is road runoff from bridge, L is Lillån stream. (For interpretation of the references to colour in this figure legend, the reader is referred to the Web version of this article.)

bridge is dewatered by drains that discharge over the banks of the stream (location R). Lillån is a natural stream that debouches into the larger stream Sagån, which in turn flows into Lake Mälaren.

2.2. Sampling procedure

Sampling was performed on the November 8, 2022, the December 16, 2022, and the March 28, 2023. The weather conditions during the sampling occasions are summarised in Table 1 and in more detail in Supplementary material A.2.

Grab samples of stormwater were collected at the different locations shown in Fig. 2B (see also Supplementary material A.1) during the occasions listed in Table 1. Water samples were retrieved using a telescopic surface water sampler and glass bottles (0.5 L or 1 L) with lids covered

internally with PTFE, apart from location D that was sampled by immersing the bottles directly. At most locations, several bottles were collected by taking consecutive samples to achieve the desired total sample volume between 1 and 5 L. In between samples, the telescopic sampler was rinsed with tap water to avoid cross-contamination between different sampling locations.

Grab samples of sediments were collected at the locations shown in Fig. 2B (see Supplementary material A.1 for more details) in November 2022 and March 2023, Table 1. The sediment samples at locations G1, G2 and WA were collected using an Ekman grab sampler. The sediments at the bottom of the outflow pipe into the ditch D, were retrieved using a metal trowel. Sediments from Lillån L were collected using a core sampler. Between 300 g and 1000 g of sediments were retrieved and placed in glass containers with plastic lids. In between samples, all

Table 1
Weather conditions during sampling occasions and in antecedent days at Testsite E18.

Sampling day & collected samples	Weather	Average temperature	Antecedent dry days	Conditions previous day	
				Precipitation [mm]	Peak intensity [mm/h]
Nov 8, 2022 morning G1, G2, WA, D and L	Dry	8 °C	0	5 mm rain	2.2
Nov 8, 2022 afternoon Only water: OA, OB and R	Rain: peak intensity 0.5 mm/h, total rain 1.4 mm	8 °C			
Dec 16, 2022 Only water: G1, G2 and WA	Dry, snow coverage	-18 °C	14 (rain) 0 (snow)	0.2 mm snow	0.3
Mar 28, 2023 G1, G2, WA, D and L	Dry, snow coverage	-3 °C	4 (rain) 0 (snow)	3 mm snow	1.9

samplers were rinsed with tap water to avoid cross-contamination.

2.3. Sample preparation and pre-treatment

2.3.1. TSS, VSS, DS and LOI analyses

All samples collected were stored in refrigerators. Prior to analysing the rubber content in the samples, TSS and VSS analyses were performed on the water samples to identify the solids content following standard SS-EN 872:2005. The samples for TSS analysis were filtered on 55 mm diameter glass fibre filters (Whatman GF/A, with pore size 1.6 μm) that had been preconditioned in a muffle furnace (Carbolite furnaces CSF 12/13) at 550 °C. Rinsing during filtration was made with ultrapure water (Fisher Scientific Accu100 Ultrapure Water System) and ethanol due to the presence of non-water-soluble substances in some of the samples. The filters, with the collected particles, were dried in aluminium cups that had also been pre-treated in a muffle furnace at 550 °C. Following the TSS analysis, the content of VSS in the filters with the dried material was determined by burning the filters and the aluminium cups for 2 h at 550 °C. The dry substance (DS) and the LOI were determined on the sediment samples in triplicates following standard SS 02 81 13 using pre-treated aluminium cups in the muffle furnace at 550 °C for 2 h. The sediment samples were dried for 20 h at 105 °C and burned at 550 °C for 2 h, and thereafter cooled in a desiccator. The storage time of the samples before the TSS/VSS and DS/LOI analyses was 2–3 months to coincide with the PYR-GC/MS analyses.

2.3.2. Sieve fractioning and sample preparation

For the water samples collected in November, aggregated samples for each location were made by taking subsamples of equal volumes from all bottles collected in that location. For the samples from standing water volumes (G1, G2 and WA) in December, it was concluded that re-suspension of the sediment occurred during sampling, affecting the particle concentration in consecutive bottles (see details in [Supplementary material C](#)). Therefore, for December and March samples, only the first retrieved bottles were used in the analysis for G1, G2 and WA. The water samples were treated in an ultrasonic bath (Bandelin RK 510H) for 30 min to break up agglomerated particles, after which they were readily shaken while retrieving subsamples for filtration, to obtain homogeneous samples. Subsamples were wet sieved using either VWR 20 μm test sieve ISO 3310 or Fisherbrand 500 μm test sieve ISO 3310, depending on the desired size fractioning. The water subsamples <500 μm with TSS content above 70 mg/L were transferred to 50 mL Falcon tubes and centrifuged (Labex Sigma 4–16, 3000 rpm/min) to ease filtration, and the supernatant was filtered first, as suggested by [Rødland et al. \(2022a\)](#), followed by resuspension of the particle fallout from the centrifugation and addition onto the same filter. Direct filtration was employed for sieved water subsamples <20 μm and <500 μm with lower TSS content. Glass filtration equipment under vacuum and binder-free glass fibre filters (GF/A, Whatman, pore size 1.6 μm , diameter 25 mm), pre-treated 2 h at 550 °C in a muffle furnace, were used for filtration, yielding a particle cut-off size of 1.6 μm . Ultrapure water and ethanol were used for rinsing during filtration. The dry filters were weighted before and after filtration, and then rolled into pyrolysis cups for analysis. Selected water samples were analysed in triplicates in November (G1, G2 and WA) and in duplicates in March (G2, WA and L; the filters used for the second replicates were accidentally subjected to longer pre-treatment in oven) to verify the homogeneity of the subsamples. Additional tests were performed to investigate the effects on TWP concentration of the pre-treatment with ultrasonication and of the prolonged sample storage before analysis on TWP concentration (see [Supplementary material C](#)). Quality assurance and quality control (QA/QC) considerations and results can be found in [Supplementary material A.4](#).

The sediment samples were stirred and shaken to obtain representative subsamples, with the procedure performed in triplicates. The subsamples were weighted and wet sieved with ultrapure water and

ethanol while brushing with a hog brush. Mesh sieves VWR 20 μm test sieve ISO 3310 and Fisherbrand 500 μm test sieve ISO 3310 were used to obtain particle size fractions <20 μm and <500 μm . The sediment subsamples <20 μm were wet sieved with plenty of liquid and treated as the water samples: part of the diluted subsample was filtered directly yielding the size fractions 1.6–20 μm . The filters were weighted, folded, rolled and put into pyrolysis cups. The sediment subsamples <500 μm were wet sieved directly into glass jars (pre-rinsed with distilled water, dried and pre-weighted) and dried in an oven (Thermo Scientific Heratherm OGS60) at 95 °C for 20 h, resulting in the size fraction 0–500 μm . The dried sediments in the jars were weighted and homogenised using a metal spoon. Small amounts of the sediment from the jars were put into pyrolysis cups and weighted (4–15 mg/cup). The SBR + BR amounts obtained from PYR-GC/MS divided by the weight of the pyrolyzed mass yielded SBR + BR concentrations over the dry weight (d.w.) of sieved sediments <500 μm (d.w. <500 μm). Using the DS results, these concentrations were also calculated as SBR + BR/total d.w. of the unsieved sediment sample (see [Supplementary material A.3](#)).

2.4. Pyrolysis GC/MS analysis

The samples were analysed for the total SBR and BR concentrations following the PYR-GC/MS methodology developed by [Rødland et al. \(2022b\)](#) using marker combinations of benzene, α -methylstyrene, ethylstyrene, and butadiene trimer. [Rødland et al. \(2022b\)](#) showed that this combination of marker compounds yielded lower variation in SBR + BR concentrations compared to other markers (4-vinylcyclohexene (4-VCH), SB dimer, and SBB trimer). SBR + BR have been shown to be present in tyres from both personal vehicles (PV) and heavy-duty vehicles (HV) ([Rauert et al., 2021](#); [Rødland et al., 2022b](#)). Natural rubber has not been used for TWP quantification, as it is difficult to measure in environmental samples due to interference from plant material ([Eisen- traud et al., 2018](#)).

Samples were analysed with a Multi-Shot Pyrolyzer (EGA/PY-3030D) equipped with an Auto-Shot Sampler (AS-1020 E) (Frontier lab Ltd., Fukushima, Japan) coupled to gas chromatography-mass spectrometer (GC/MS) (5977 B MSD with 8860 GC, Agilent Technologies Inc., CA, USA), following the method of [Rødland et al. \(2022b\)](#) with modifications (see detailed settings in [Supplementary material A.5](#)). Calibration was performed using SBR1500 (Polymer Source Inc., Canada) in solution (chloroform, Sigma Aldrich) and internal standard (deuterated polybutadiene, d_6 -PB, in chloroform solution). Calibration points (1, 5, 20, 60, 120 and 140 $\mu\text{g}/\text{cup}$) were analysed in triplicates. Quantification was performed using two marker combinations for SBR + BR: combination *a* consisted of m/z 78 Da for benzene, m/z 118 Da for α -methylstyrene, m/z 117 Da for ethylstyrene, and m/z 91 Da for butadiene trimer (calibration curve $R^2 = 0.99$), and combination *b* consisted of the same markers as *a* but without benzene (m/z 78) (calibration curve $R^2 = 0.98$). The ratio between the four markers was monitored in each sample and compared to the ratios in the SBR1500 calibration samples and to previous ratios found for commercial tyres ([Rødland et al., 2022b](#)). The asphalt on the highway contains residues of polymer modified bitumen (PMB) asphalt (see section 2.1), meaning that traces of styrene-butadiene styrene (SBS) might be present in the samples which would be identified as SBR + BR during analysis. As the SBS amount from the PMB asphalt is expected to be low compared to SBR + BR from tyre wear, quantification was performed by only using SBR1500.

In samples with high organic matter content and complex matrix, there is a possibility of marker interference from additional sources of benzene ([Rødland et al., 2023b](#)). By using the expected ratios as a control, in samples where the benzene contribution is higher than expected, benzene is removed as a marker for that specific sample and quantification is made using combination *b* (see marker used per sample in [Supplementary material A.4](#)). The 4-VCH marker for butadiene rubber (SBR + BR) was monitored as a control, as it is less impacted by

potential competing sources from the matrix, but was not used for quantification due to higher variability in commercial tyres compared to marker combination *a*.

2.5. Calculations of tyre wear particle concentrations

Calculation of TWP followed the procedures described by Rødland et al. (2022b) (Equation (1)). The TWP concentration in each sample was calculated 100,000 times by Monte Carlo simulation (software Oracle Crystal Ball in Microsoft Excel) using Equation (1) to estimate the mean value of M_T to account for the variability of SBR + BR content in different types of tyres. The measured SBR + BR value in the sample (M_{SB}) was adjusted by a conversion factor (S_C) of 0.94 to adjust for the difference in styrene content of SBR1500 (23%, Polymer Source Inc.) versus average styrene content in commercial tyres (15% (Unice et al., 2013, 2012);). The range of SBR + BR concentrations in tyres of PV and HV was based on a database developed by Rødland et al. (2022b) and was adjusted according to the ratios of different vehicle types at Testsite E18 (R_{PV} and R_{HV}).

$$M_T = \frac{M_{SB} \cdot S_C}{(S_{PV} \cdot R_{PV}) + (S_{HV} \cdot R_{HV})} \quad (1)$$

where.

- M_T - mass of tyre in a sample [mg];
- M_{SB} - mass of SBR + BR found using PYR-GC/MS in the sample [μg];
- S_C - conversion factor for styrene content;
- S_{PV} - mean mass of SBR + BR in PV [$\mu\text{g}/\text{mg}$] from a database developed by Rødland et al. (2022b);
- R_{PV} - ratio of PV at the sampling location - value 0.9 based on traffic data;
- S_{HV} - mean mass of SBR + BR in HV [$\mu\text{g}/\text{mg}$] from a database developed by Rødland et al. (2022b);
- R_{HV} - ratio of HV at the sampling location - value 0.1 based on traffic data.

3. Results and discussion

First, concentrations of SBR + BR in water and sediment samples are presented. These results are compared between different sampling locations and occasions, as well as between the analysed size fractions. Thereafter, the median TWP concentrations, calculated through the Monte Carlo simulation, are presented and discussed in relation to values reported in literature.

3.1. Water samples

3.1.1. Styrene-butadiene rubbers in water: size fraction 1.6–500 μm

The SBR + BR concentrations found in the water samples are presented in Fig. 3A. The replicates showed only small variation in concentration. There were no statistically significant differences in concentrations between the three sampling occasions (November, December, and March; unpaired samples *t*-test, $p > 0.1$). Within the stormwater system, the measured concentrations of SBR + BR were lower in the first gully pot (G1) compared to the second gully pot (G2) with a weak significance (linear regression corrected for triplicates, $p = 0.054$). The higher concentration in G2 in November 2022 can be explained by resuspension during sampling with consecutive bottles, due to a high sediment level in gully pot G2 (see Supplementary material C.1). The concentration of SBR + BR decreased in the collecting well A (WA) to which both G1 and G2 drain, with a significant difference between G2 and WA (linear regression corrected for triplicates, $p = 0.004$). One explanation for the lower SBR + BR concentration in the water from WA is the larger volume of the well, which could promote sedimentation of the particles and prevent resuspension.

The second section of the stormwater system, sampled in November and March, consisted of water that drains into the ditch and Lillån (D and L in Fig. 2). The water in the ditch by the outlet is discharged from the wells collecting water from the gully pots, from the geo-textile ditches at the sides of the road, and partly from the adjacent highway.

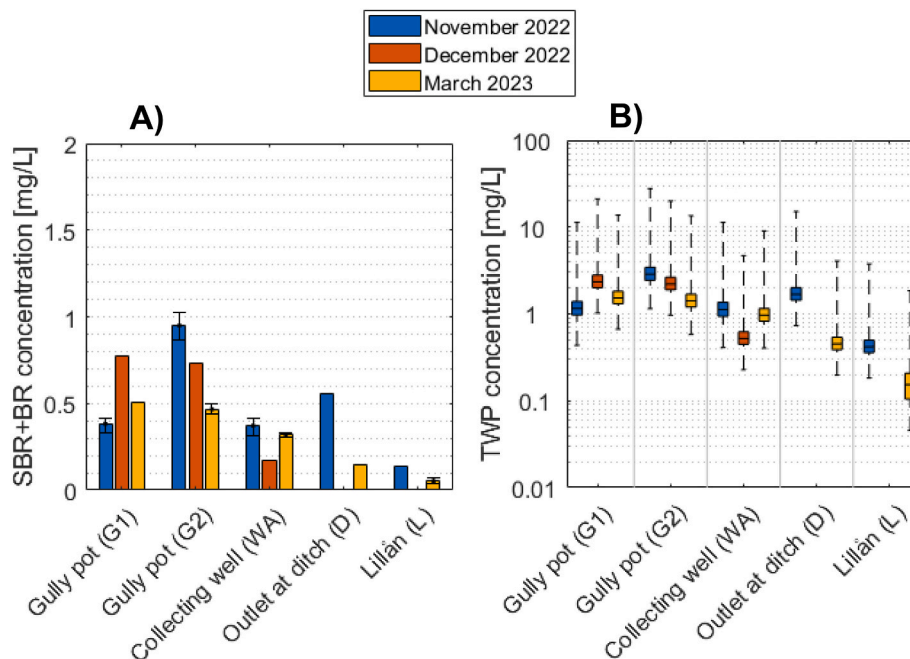


Fig. 3. A) Bar chart of the measured concentrations of SBR + BR in the water samples for the size fraction 1.6–500 μm . Note that for December 2022 only G1, G2, and WA were sampled. Error bars representing maximum and minimum values of the replicates are plotted for the samples analysed in triplicates (G1, G2 and WA from November 2022) and duplicates (G2, WA and L from March 2023). B) Box chart of the calculated TWP concentration in the water samples for the size fraction 1.6–500 μm . The median value of the TWP calculations is plotted, and the box edges represent the 25th and 75th percentiles of TWP calculation. The whiskers show the maximum and minimum values of the TWP calculation. Note that for December 2022 only G1, G2, and WA were sampled. (For interpretation of the colour in this figure legend, the reader is referred to the Web version of this article.)

Overall, the concentration in the ditch was similar to the first section of the stormwater system: in March D had lower SBR + BR concentrations, whereas in November, D had a higher concentration than G1 and WA, but lower than G2. Lower concentrations of SBR + BR were found in the stream Lillån L compared to the other locations (0.05 mg/L in March using marker *b* and 0.14 mg/L in November). The minimum concentration in Lillån in March was only 22% higher than the largest SBR + BR amounts in the blanks. However, 4-VCH was 219% higher than in the blanks, and the SBR + BR concentration in November was 280% larger than in the blanks (see [Supplementary material A.4](#)), confirming the presence of SBR + BR in the stream water. This is in agreement with the classification of the Lillån stream as being considerably affected by transport and infrastructure ([Water Information System Sweden, 2024](#)).

Results for locations R (runoff directly from the road surface), and outflowing water from the wells OA and OB can be found in [Supplementary material B.1](#). Locations R and OA were sampled in November 2022 when a light rain generated runoff flow. The water draining from the bridge (R) during the rain event had the highest concentration of SBR + BR, 5.6 mg/L, among all water samples, indicating mobilization of TWP from the road surface. The outflow water from well A (OA) also demonstrated a high SBR + BR concentration of 3.5 mg/L, but it cannot be assessed whether this is due to high SBR + BR concentration in the runoff or due to resuspension by turbulence from the runoff or by the antecedent sampling. The geo-textile ditch (OB) had a continuous outflow in November and was sampled on that occasion. However, TWP was not confirmed in OB, as the SBR + BR concentration was comparable to that of the blank tests, and 4-VCH was not detected ([Supplementary material A.4](#)).

3.1.2. Styrene-butadiene rubbers in water: size fraction 1.6–20 µm

The SBR + BR concentrations for the finer size fraction 1.6–20 µm ranged between 0.03 and 5.5 mg/L ([Supplementary material B.1](#) and [B.2](#)). This is similar to the concentrations in fraction 1.6–500 µm. The effect of the pre-treatment process of ultrasonication was investigated, and it was shown that the ultrasonication step affected the concentration of SBR + BR in the fine size fraction 1.6–20 µm ([Supplementary material C.2](#)). The ultrasonication step likely caused the breakup of mineral encrustations, which have been reported to be common for TWP ([Järskog et al., 2022b](#); [Kreider et al., 2010](#)), yielding more TWP in the size fraction 1.6–20 µm.

The mean ratio of SBR + BR 1.6–20 µm to SBR + BR 1.6–500 µm was 80% and 60% with and without ultrasonication, respectively. Thus, a large fraction of the SBR + BR concentration stems from SBR + BR in size fraction 1.6–20 µm. However, this ratio differs between the sampling locations: the proportion of SBR + BR 1.6–20 µm over SBR + BR 1.6–500 µm was largest in R and OA (>97%), whereas in the standing water volumes (G1, G2, WA, D and L), it ranged between 42 and 93%. The larger ratio of fine particles in R and OA could be explained by the rainfall and the sampling in the well only mobilising the finer TWP for further transport.

3.1.3. TSS and VSS results and correlation with SBR + BR concentrations

The results for TSS and VSS for the water samples can be found in [Supplementary material B.7](#). A strong correlation was found between the TSS and the SBR + BR concentrations both for the SBR + BR in the size fraction 1.6–500 µm ($r = 0.872$, $p < 0.001$ using Pearson correlation coefficient) and in the size fraction 1.6–20 µm ($r = 0.861$, $p < 0.001$). The correlation between VSS and SBR + BR concentration was even stronger ($r = 0.933$, $p < 0.001$ for SBR + BR 1.6–500 µm and $r = 0.927$, $p < 0.001$ for SBR + BR 1.6–20 µm). Correlation plots can be found in [Supplementary material B.9](#). These results are in line with the findings of [Rødland et al. \(2022a\)](#) who also showed a strong correlation between TSS and TWP in tunnel wash water. This strengthens the suggestion by [Rødland et al. \(2022a\)](#) of TSS as an indicator for TWP in runoff from roads, even if it might only be valid depending on specific site conditions. TSS varied from 5.1 mg/L in D up to 310 mg/L in R with an

average of 61 mg/L in the first section of the stormwater system (G1, G2 and WA). There was no statistically significant difference in TSS between the sampling campaigns (unpaired samples *t*-test $p > 0.1$). TSS concentrations are in line with the results found by [Winston et al. \(2023\)](#) in road runoff collected from catch basins draining roads enclosed by kerbstones: mean concentrations 13–70 mg/L with a maximum of 312 mg/L with no clear seasonal change. VSS values were between 0.64 mg/L (D) and 90 mg/L (R), with an average of 11 mg/L over the first section of the stormwater system. Organic matter (VSS) made on average up 21% of the solids in the samples.

3.2. Sediment samples

3.2.1. Styrene-butadiene rubbers in sediment: size fraction <500 µm

The SBR + BR concentrations in the sediments sampled in the gully pots G1 and G2, the collecting well WA, the ditch D and Lillån L are presented in [Fig. 4](#). The error bars demonstrate the heterogeneity of the gully pots' sediments, which makes it challenging to obtain representative samples. The size distribution of the sediments varied greatly between the locations, with G1, G2, and WA containing large amounts of small gravel >1 mm in November (see [Supplementary material B.10](#)), likely because the sediments with larger grain sizes are not easily transported further in the stormwater system. Therefore, the SBR + BR concentrations <500 µm are presented in two different ways in [Fig. 4A](#) and [Fig. 4B](#). In [Fig. 4A](#), the concentration is calculated by dividing by the total d.w. of the unsieved sediments, and the total d.w. of the unsieved sediments was calculated using the DS results. Meanwhile, in [Fig. 4B](#), the calculation is based on d.w. <500 µm of the sieved fraction.

A weak significant difference between the sampling occasions was identified when using the SBR + BR concentrations based on the total d.w., where March presented higher SBR + BR concentrations compared to November 2022 (un-paired samples *t*-test, $p = 0.053$). There was no significant difference between the sampling occasions when using the concentrations based on d.w. <500 µm (un-paired samples *t*-test, -0.430 , $p = 0.793$). The sediments in the gully pots G1 and G2 had lower SBR + BR concentrations in November compared to March, [Fig. 4A](#). No significant difference between the gully pots G1 and G2 was identified. A significant difference between the gully pot (G1 and G2, respectively) and WA was identified when dividing with total d.w. (linear regression, corrected for triplicates, $p < 0.1$ and $p < 0.01$, respectively), but not with d.w. <500 µm. Sediments from the outlet pipe at the ditch (D) had significantly higher concentrations than sediments in the stormwater system (G1, G2, WA) both when looking at SBR + BR concentrations based on total d.w. ($p < 0.01$, $p < 0.001$, and $p < 0.1$, respectively) and based on d.w. <500 µm ($p < 0.05$ for all). The ditch receives water from several sources (see section 2.1), which may contribute to the identified difference. Another possible explanation is that the volumes of G1, G2, and WA predominantly retain coarser and more dense sediments, but not the finer sediments in which TWP is mostly present, as TWP is primarily reported to be finer than 200 µm ([Klößner et al., 2021](#); [Kreider et al., 2010](#)). This could lead to higher relative TWP concentration over the total mass of sediments further downstream. This is evident from the mass of sediments in different size ranges which can be found in [Supplementary material B.10](#). It can be seen that location D had more fine material (on average 22.5% in size range 1.6–20 µm) compared to other locations, except for Lillån L. A last hypothesis is that at the outlet pipe at the ditch D, which was partially submerged by the small standing water volume in the ditch during sampling, the particles experience extended retention time during dry weather that could benefit the settling of TWP.

3.2.2. Styrene-butadiene rubbers in sediment: size fraction 1.6–20 µm

There is no significant difference in SBR + BR concentrations in the size 1.6–20 µm between the sampling locations gully pots G1 and G2, collecting well WA, and the outlet at ditch D, when calculated with the denominator d.w. <500 µm (linear regression corrected for triplicates).

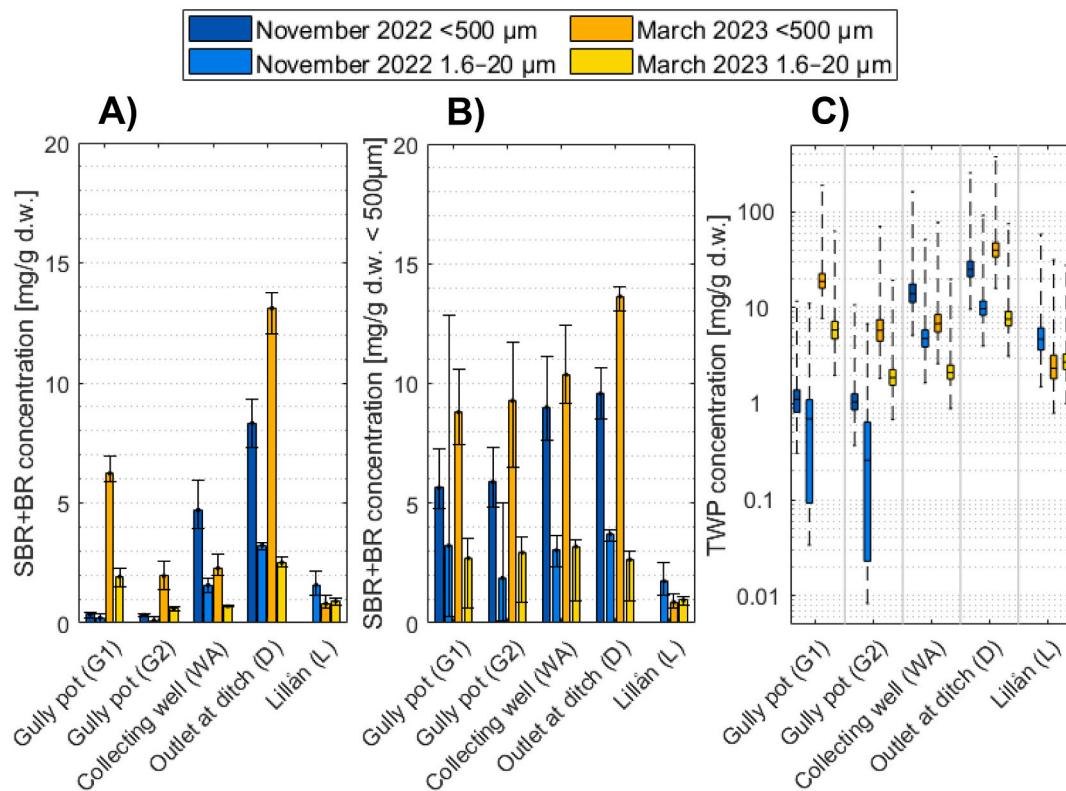


Fig. 4. A) Bar chart of the measured mean concentration of SBR + BR in the sediment samples over the total unsieved samples dry weight (d.w.) collected in November 2022 and March 2023 for the size fractions $<500\ \mu\text{m}$ and $1.6\text{--}20\ \mu\text{m}$. Error bars represent maximum and minimum values of the replicates. The bars are missing for the samples in which SBR + BR was not found. B) Bar chart of the measured mean concentration of SBR + BR in the sediment samples presented as concentrations over d.w. of the samples $<500\ \mu\text{m}$ (d.w. $<500\ \mu\text{m}$). Error bars represent maximum and minimum values of the replicates. The bars are missing for the samples in which SBR + BR was not found. C) Box charts of the calculated TWP concentrations. The median value of the TWP calculations is plotted, and the box edges represent the 25th and 75th percentile of TWP calculation. The whiskers show the maximum and minimum calculated concentrations of TWP. The bars are missing for the samples in which SBR + BR was not found. (For interpretation of the colour in this figure legend, the reader is referred to the Web version of this article.)

When dividing with total d.w., the outlet pipe at ditch D has a significantly higher concentration of SBR + BR $1.6\text{--}20\ \mu\text{m}$ compared to G1, G2, and WA, respectively ($p < 0.01$, $p < 0.001$, and $p < 0.001$). WA has a significantly higher concentration compared to G2, if using the denominator total d.w. ($p < 0.05$). This indicates that TWP in this size does not settle to a large extent in the gully pots, or that TWP is resuspended easily and transported downstream at higher stormwater flows. In November, SBR + BR was found in the size fraction $1.6\text{--}20\ \mu\text{m}$ for Lillån L, but not in the size fraction $<500\ \mu\text{m}$. An explanation could be that mostly fine TWP is transported to the river, and that removing sediments $>20\ \mu\text{m}$ by wet sieving enriched the TWP concentration in the sample and removed material that could interfere with the analysis, allowing the quantification of SBR + BR.

In all sediment samples, the finer size fraction accounts for an important mass fraction of the SBR + BR detected: 20–60% of the SBR + BR mass was found in the size fraction $1.6\text{--}20\ \mu\text{m}$ in the samples from the stormwater system (G1, G2, WA, and D). This agrees with the mass ratios 20–40% of TWP $<20\ \mu\text{m}$ reported by Klöckner et al. (2020) for sediments in sedimentation basins. Kreider et al. (2010) found that the size distribution of TWP generated in a road simulator laboratory had a mode at $75\ \mu\text{m}$, which is coarser than what is suggested by the current study. However, later research also suggests the abundance of finer particle sizes: Kovichich et al. (2021) reported that TWP generated in a road simulator ranged between 6 and $120\ \mu\text{m}$ with a mode at $34\ \mu\text{m}$, while Klöckner et al. (2021) suggested a mode in the finest size fraction $<20\ \mu\text{m}$ for road dust from German tunnels. It should also be considered that TWP in environmental samples are likely subjected to additional weathering processes compared to particles generated in laboratory

settings. The abundance of TWP in the smaller size fraction is interesting as the fraction below $<30\ \mu\text{m}$ is suggested to not being prone to sedimentation (Vogelsang et al., 2019), and further studies on this topic are needed to understand the processes behind.

3.2.3. LOI results

The LOI results can be found in [Supplementary material B.8](#). The samples from the outlet at the ditch D had the highest content of organic matter, with an average of 15%. Linear regression, corrected for triplicates, showed significant difference between the first part of the stormwater system (G1, G2, and WA) compared to D ($p < 0.05$, $p < 0.01$, and $p < 0.01$), and between G2, WA, and D compared to Lillån L ($p < 0.001$, $p < 0.05$, and $p < 0.01$). There was a strong correlation between LOI and the SBR + BR concentration over total d.w., both when comparing the SBR + BR concentration $<500\ \mu\text{m}/\text{d.w.}$ ($r = 0.72$, $p = 0.001$ using Pearson correlation coefficient) and the SBR + BR concentration $1.6\text{--}20\ \mu\text{m}/\text{d.w.}$ ($r = 0.91$, $p = 0.0001$). Correlation plots can be found in [Supplementary material B.9](#).

3.3. Comparison of TWP concentrations in water and sediment samples

The TWP concentration distributions for water ($1.6\text{--}500\ \mu\text{m}$) and sediment samples ($<500\ \mu\text{m}$) are presented in [Fig. 3C](#) and [Fig. 4C](#), respectively. The TWP concentrations are based on SBR + BR content of summer tyres and winter tyres (studded and non-studded) for both personal and heavy-duty vehicles. The median, standard deviation, and percentiles of the obtained TWP concentrations from the Monte Carlo simulation are listed in [Supplementary material B.5](#) and [B.6](#) to account

for the large variability of SBR + BR content in tyres. For the purpose of comparing the TWP concentrations with other studies, the median TWP concentration is used. The median TWP concentration in road runoff R, 17 mg/L, and in the outflow from well OA, 10 mg/L, are in line with results from previous studies on tunnel wash water and direct runoff from a German highway, although in the lower range of the reported values, Table 2. TWP concentrations in the standing water volumes of the gully pots G1 and G2, and well WA, 0.52–2.9 mg/L, and outlet at the ditch D, 0.45–1.7 mg/L, are similar to reported concentrations in stormwater drains and retention ponds, Table 2. The TWP concentrations in Lillån stream, 0.15–0.42 mg/L, were in between the values found in rivers and surface waters in other studies, Table 2.

The TWP concentrations in the sediment phase in the particle fraction <500 µm were 1.0–19 mg/g in the sediments of the gully pots (G1 and G2), and 6.8–14 mg/g and 25–40 mg/g in the collecting well (WA) and at the outlet of the stormwater system (D), respectively. These results are in line with previously measured concentrations in gully pots in cities and in a road tunnel, and in sedimentation ponds, Table 2. The TWP concentrations in Lillån sediments L, 2.3–4.7 mg/g, were similar to those reported in rivers, but higher than in a lake, Table 2. Comparisons of concentrations between studies are difficult because of the different analysis methods, studied particle sizes, and analytical challenges associated with the quantification of TWP (Rødland et al., 2023a). In addition, the ambient concentrations depend on current and antecedent weather conditions and on traffic volumes, driving behaviour, tyre composition, and road surface roughness (Andersson-Sköld et al., 2020;

Table 2

TWP concentrations reported by earlier studies together with the analysis method employed by the studies and the size range of the identified TWP based on the sampling pre-treatment used in the studies.

Study	Sample type	Size fraction	Analysis method	TWP concentration
Water samples				
Rødland et al. (2022a)	Untreated tunnel wash water	>1.6 µm	PYR-GC/MS	14.5–47.8 mg/L
Drøge and Tromp (2019)	Runoff from highway road side	No reported size range	TED-GC/MS	51–59 mg/L
Rauert et al. (2022)	Stormwater drain water	>1 µm	PYR-GC/MS	231–665 µg/L ^a
Rauert et al. (2022)	Retention pond water	>1 µm	PYR-GC/MS	72–236 µg/L ^a
Drøge and Tromp (2019)	Surface waters	No reported size range	TED-GC/MS	0.001–0.011 mg/L
Rauert et al. (2022)	Creeks and rivers in urban centres	>1 µm	PYR-GC/MS	<MDL–480 µg/L ^a
Sediment samples				
Mengistu et al. (2021)	Urban gully pot	<5 mm	STA-FTIR + PARAFAC	0.8–149.6 mg/g sediment d.w.
Rødland et al. (2022a)	Gully pots in road tunnel	<1 mm	PYR-GC/MS	4.75–53.1 mg/g
Klößner et al. (2020)	Sedimentation ponds	<500 µm	TED-GC/MS	0.95–11 mg/g ^a
Unice et al. (2013)	River	<1 mm	PYR-GC/MS	13–3700 µg/g d.w. ^a
Barber et al. (2024)	River	<5 mm ^b	PYR-GC/MS	45–1150 mg/kg ^a
Klößner et al. (2020)	Lake	<500 µm	TED-GC/MS	0.085 mg/g ^a

^a The presented reported values from the studies have been adjusted by dividing by two to convert from tyre and road wear particle concentration to tyre tread concentration.

^b Overlying water in trap sediment samples was decanted and filtered on 0.45 µm filters and the material on the filter was re-added to the sediments.

Kole et al., 2017).

3.3.1. Comparison to previous TWP measurements at testsite E18

There are two previous studies at Testsite E18 (Drøge and Tromp, 2019; Järslkog et al., 2022a), and their results are summarised in Table 3 together with the results from this study. Järslkog et al. (2022a) analysed water and sediment grab samples from gully pot G2 and collecting well WA, using automated Scanning Electron Microscopy/Energy Dispersive X-ray spectroscopy (SEM/EDX) coupled with a machine learning algorithm for identification of tyre wear. The analysed size fractions were 20–125 µm and 2–20 µm.

In Table 3 it can be seen that Järslkog et al. (2022a) detected larger amounts of TWP and bitumen in both water and sediments for the finer size fraction (size fraction 2–20 µm) compared to this study (1.6–20 µm), especially in collecting well WA. The higher concentrations can partly be explained by the analysis method of Järslkog et al. (2022a) not differentiating between tyre and bitumen in the lower size fraction. Regarding the coarser size fraction, similar concentrations were found in the sediments of both locations. The fact that this study has an upper cut-off of 500 µm, instead of 125 µm as Järslkog et al. (2022a) had, is not expected to affect the comparison significantly, as TWP is reported to mostly be present in size fractions below ca 200 µm (Klößner et al., 2021; Kreider et al., 2010). In the water phase, Järslkog et al. (2022a) found higher concentrations of TWP in the coarser size fraction compared to this study. The explanation for the differences could be the different weather conditions, where Järslkog et al. (2022a) had 10 antecedent dry days preceded by about 3 mm accumulated precipitation, whereas weather conditions from the present study are summarised Table 1. For the water samples, it was seen that resuspension of TWP easily occurred when sampling (see Supplementary material C.1), which could yield different results. In addition, the SEM/EDX analysis method employed by Järslkog et al. (2022a) is a powerful tool for the quantification, characterisation, and classification of individual particles, but it does not allow exact absolute mass quantification (Järslkog et al., 2022a).

The TWP concentrations in collecting well (WA) at Testsite E18, were also estimated by Drøge and Tromp (2019) using Thermal extraction and desorption GC/MS (TED-GC/MS) with marker compounds 4-vinylcyclohexene, styrene, and dipentene together with conversion factors to tyre mass based on Dutch traffic data. They found 1 mg/L of tyre wear in the water phase and 13 mg/g in the sediment phase, which are well in line with the findings in this study, Table 3.

3.4. Concluding discussion

This work has addressed the characterisation of TWP concentration in both water and sediments of a highway stormwater system. There is little knowledge about environmental concentrations, retention, and sedimentation of TWP (Gehrke et al., 2023). Hence, the work contributes to increased knowledge on TWP concentrations and spread in a highway environment. This work demonstrates varying TWP concentrations following the stormwater path from the road surface to the receiving waters. The sampling campaign is limited in time, as it consists of grab samples collected on three occasions, and for future studies, to fully address the transport of TWP in the near-road environment during rain events, continuous monitoring of TWP is needed.

In this study, the TWP concentrations were analysed using PYR-GC/MS, which made it possible to quantify the fine particles <20 µm that were often neglected in previous studies. However, using PYR-GC/MS, it is not possible to assess the morphology or the sizes of the particles in more detail (Rødland et al., 2023a). For future work, complementary imaging techniques, such as SEM-EDX, could provide increased knowledge on the number of TWP in fine-size fractions in more detail (>1 µm) and on the morphology of the particles. However, challenges still exist for SEM-EDX techniques to differentiate between TWP and bitumen for particles <20 µm (Järslkog et al., 2022b) and to identify less pristine TWP (Rødland et al., 2023a). The investigation of the pre-treatment of

Table 3

Comparison of tyre wear particles (TWP) concentrations determined in different studies and with different analysis methods at Testsite E18.

	Gully pot (G2)			Collecting well (WA)		
	Water [mg/L]	Sediment [mg/g]	Size fractions	Water [mg/L]	Sediment [mg/g]	Size fractions
PYR-GC/MS + Monte Carlo simulation ^a	1.1 ^d ; 2.1 ^c ; 2.2 ^b 1.4 ^d ; 2.2 ^c ; 2.9 ^b	0.26 ^b ; 1.9 ^d 1.0 ^b ; 5.8 ^d	1.6–20 µm 1.6–500 µm	0.82 ^d ; 0.94 ^b 0.52 ^c ; 0.97 ^d ; 1.1 ^b	2.1 ^d ; 4.8 ^b 6.8 ^d ; 14 ^b	1.6–20 µm 1.6–500 µm
Calculated difference between concentrations ^e	0.2–0.7	0.8–4	20–500 µm	0.1–0.2	5–9	20–500 µm
Järalskog et al. (2022a) SEM-EDX + calculations	10	21.4	2–20 µm TWP + bitumen	150	71	2–20 µm TWP + bitumen
Dröge and Tromp (2019) TED-GC/MS + conversion factor	10 Not analysed	3.5 Not analysed	20–125 µm –	130 1.0	14.5 13	20–125 µm No reported cut-off

^a The TWP concentrations for the current paper (November and December 2022, and March 2023) are presented as the median of the Monte Carlo simulation rounded to two significant figures.

^b Results from sampling in November 2022.

^c Results from December 2022.

^d Results from March 2023.

^e The results in the size fraction 20–500 µm have been calculated by subtracting the TWP concentration 1.6–20 µm from the TWP concentration <500 µm.

the water samples demonstrated that ultrasonication increased the proportion of finer particles. SEM-EDX analysis could help assess whether this was caused by the disaggregation of mineral encrustations as hypothesized.

This study focused on the transport of TWP through a stormwater system. Along many highways, including most parts of E18, the road surface is dewatered directly into roadside ditches. Consequently, to further understand the spread and occurrence of TWP along highways, soil samples should be analysed. One implication of this work is that TWP was detected in the nearby river, indicating that TWP is spread to receiving waters. This study cannot confirm the pathway through which the TWP was transported to the river, since TWP can be transported through the stormwater system, as well as through the air (Goßmann et al., 2023) and by other sources and pathways (Andersson-Sköld et al., 2020). More work should be put to assess the contribution of different TWP pathways to the environment, and numerical modelling could help to estimate their relative contribution.

The abundance of TWP in size fraction <20 µm and the high TWP concentrations found downstream of the gully pots indicate that gully pots are ineffective in retaining TWP in their sand traps. As particles <30 µm do not sediment in gully pots due to the short retention time (Vogelsang et al., 2019), and since some laboratory studies suggest that transport of hydrophobic stormwater pollutants occurs in the form of emulsions (Markiewicz et al., 2019), it is unlikely that stormwater solutions based on sedimentation would be efficient for limiting the spread of TWP. Limited removal of microplastics is hypothesized for traditional stormwater solutions such as constructed wetlands (Monira et al., 2021) and gross pollutant traps (Lange et al., 2022), whereas studies on porous asphalt (Mitchell et al., 2023; Rasmussen et al., 2023) and bioretention filters (Johansson et al., 2024) show some promising results. However, to fully assess the treatment efficiency of gully pots for TWP, the transient behaviour of TWP during rain events should be investigated.

4. Conclusions

In this study, water and sediment were sampled at selected points in a stormwater system of a Swedish highway. The samples were analysed for styrene-butadiene rubber concentrations from which concentrations of tyre wear particles (TWP) were calculated. Suspended solids were analysed for the water samples and organic content was analysed for the sediment samples. The main conclusions are that:

- TWP was found in almost all locations sampled, with concentrations up to 17 mg/L in the water samples and up to 40 mg/g in the sediment samples.

- High TWP concentration in road runoff suggests their high mobility in the water phase, supported by easy resuspension of TWP in standing water volumes.
- In the sediment samples, TWP in the size fraction 1.6–20 µm represented a significant proportion of the TWP (20–60%).
- TWP content in the sediments was significantly higher at the end of the stormwater system than at the beginning, indicating that sand trap volumes of the investigated gully pots are insufficient to fully retain tyre wear.
- A strong correlation was found between TWP concentrations in water and TSS and VSS, respectively, and between TWP content and organic content in the sediments (LOI).

Further research should investigate potential differences in tyre wear quantification from various analytical techniques to facilitate comparison between studies using different methods. Also, transient concentration changes of TWP during rain events should be investigated to understand its behaviour in stormwater systems under varying weather conditions.

Funding

This work was supported by the Swedish Research Council FORMAS, [2019–00284]; the Norwegian Public Roads Administration [B11191 Ferjefri E39]; J. Gust. Richert foundation [2022–00807], Sveriges Ingenjörer Environmental fund [2022]; Adlerbertska Research foundation [2022]; Åke and Greta Lissheds foundation [2022–00188].

Declaration of generative AI in scientific writing

During the preparation of this work the author(s) used ChatGPT 3.5 OpenAI in order to improve readability of the text. After using this tool/service, the author(s) reviewed and edited the content as needed and take(s) full responsibility for the content of the publication.

CRediT authorship contribution statement

Elly Lucia Gaggini: Writing – review & editing, Writing – original draft, Visualization, Validation, Methodology, Investigation, Funding acquisition, Formal analysis, Conceptualization. **Maria Polukarova:** Writing – review & editing, Methodology, Investigation. **Mia Bonde-lind:** Writing – review & editing, Supervision, Project administration, Methodology, Funding acquisition, Conceptualization. **Elisabeth Rødland:** Writing – review & editing, Methodology, Investigation, Formal analysis. **Ann-Margret Strömvall:** Writing – review & editing,

Methodology. Yvonne Andersson-Sköld: Writing – review & editing, Supervision, Methodology, Conceptualization. Ekaterina Sokolova: Writing – review & editing, Supervision, Project administration, Methodology, Investigation, Funding acquisition, Formal analysis, Conceptualization.

Declaration of competing interest

The authors declare that they have no known competing financial interests or personal relationships that could have appeared to influence the work reported in this paper.

Data availability

Data will be made available on request.

Acknowledgements

The Swedish Road Administration for support on Testsite E18 and for providing weather and traffic data. Aniruddha Kshirsagar for assisting during the field sampling. Niels Markwat for assistance with statistical analysis of the data. Amir Saeid Mohammadi for helping with the laboratory work.

Supplementary material

Supplementary data to this article can be found online at <https://doi.org/10.1016/j.jenvman.2024.121989>.

References

- Andersson-Sköld, Y., Johansson, M., Gustafsson, M., Järnskog, I., Lithner, D., Polukarova, M., Strömvall, A.M., 2020. Microplastics from Tyre and Road Wear - A Literature Review (No. VTI: 2018/0038-7.2), VTI Rapport 1028A.
- Barber, T.R., Claes, S., Ribeiro, F., Dillon, A.E., More, S.L., Thornton, S., Unice, K.M., Weyrauch, S., Reemtsma, T., 2024. Abundance and distribution of tire and road wear particles in the Seine River, France. *Sci. Total Environ.* 913 <https://doi.org/10.1016/j.scitotenv.2023.169633>.
- Dröge, R., Tromp, P., 2019. CEDR call 2016: environmentally sustainable roads: surface- and groundwater quality. CEDR Conference of European Directors of Roads.
- Eisenbraun, P., Dümichen, E., Ruhl, A.S., Jekel, M., Albrecht, M., Gehde, M., Braun, U., 2018. Two Birds with One Stone - Fast and Simultaneous Analysis of Microplastics: Microparticles Derived from Thermoplastics and Tire Wear. *Environ. Sci. Technol. Lett.* 5, 608–613. <https://doi.org/10.1021/acs.estlett.8b00446>.
- Gehrke, I., Schläfle, S., Bertling, R., Öz, M., Gregory, K., 2023. Review: mitigation measures to reduce tire and road wear particles. *Sci. Total Environ.* 904, 166537 <https://doi.org/10.1016/j.scitotenv.2023.166537>.
- Goßmann, I., Herzke, D., Held, A., Schulz, J., Nikiforov, V., Georgi, C., Evangelou, N., Eckhardt, S., Gerds, G., Wurl, O., Scholz-Böttcher, B.M., 2023. Occurrence and backtracking of microplastic mass loads including tire wear particles in northern Atlantic air. *Nat. Commun.* 14 <https://doi.org/10.1038/s41467-023-39340-5>.
- Järnskog, I., Jaramillo-Vogel, D., Rausch, J., Gustafsson, M., Strömvall, A.M., Andersson-Sköld, Y., 2022a. Concentrations of tire wear microplastics and other traffic-derived non-exhaust particles in the road environment. *Environ. Int.* 170, 107618 <https://doi.org/10.1016/j.envint.2022.107618>.
- Järnskog, I., Jaramillo-Vogel, D., Rausch, J., Perseguers, S., Gustafsson, M., Strömvall, A.M., Andersson-Sköld, Y., 2022b. Differentiating and quantifying carbonaceous (tire, bitumen, and road marking wear) and non-carbonaceous (metals, minerals, and glass beads) non-exhaust particles in road dust samples from a traffic environment. *Water Air Soil Pollut.* 233, 1–24. <https://doi.org/10.1007/s11270-022-05847-8>.
- Järnskog, I., Strömvall, A.M., Magnusson, K., Gustafsson, M., Polukarova, M., Galfi, H., Aronsson, M., Andersson-Sköld, Y., 2020. Occurrence of tire and bitumen wear microplastics on urban streets and in sweepings and washwater. *Sci. Total Environ.* 729 <https://doi.org/10.1016/j.scitotenv.2020.138950>.
- Johansson, G., Fedje, K.K., Modin, O., Haeger-Eugensson, M., Uhl, W., Andersson-Sköld, Y., Strömvall, A.M., 2024. Removal and release of microplastics and other environmental pollutants during the start-up of bioretention filters treating stormwater. *J. Hazard Mater.* 468 <https://doi.org/10.1016/j.jhazmat.2024.133532>.
- Klöckner, P., Seiwert, B., Eisenbraun, P., Braun, U., Reemtsma, T., Wagner, S., 2020. Characterization of tire and road wear particles from road runoff indicates highly dynamic particle properties. *Water Res.* 185, 116262 <https://doi.org/10.1016/j.watres.2020.116262>.
- Klöckner, P., Seiwert, B., Weyrauch, S., Escher, B.I., Reemtsma, T., Wagner, S., 2021. Comprehensive characterization of tire and road wear particles in highway tunnel road dust by use of size and density fractionation. *Chemosphere* 279. <https://doi.org/10.1016/j.chemosphere.2021.130530>.
- Knight, L.J., Parker-Jurd, F.N.F., Al-Sid-Cheikh, M., Thompson, R.C., 2020. Tyre wear particles: an abundant yet widely unreported microplastic? *Environ. Sci. Pollut. Control Res.* 27, 18345–18354. <https://doi.org/10.1007/s11356-020-08187-4>.
- Kole, P.J., Löhr, A.J., Van Belleghem, F.G.A.J., Ragas, A.M.J., 2017. Wear and tear of tyres: a stealthy source of microplastics in the environment. *Int. J. Environ. Res. Publ. Health* 14. <https://doi.org/10.3390/ijerph14101265>.
- Kovochich, M., Liong, M., Parker, J.A., Oh, S.C., Lee, J.P., Xi, L., Kreider, M.L., Unice, K.M., 2021. Chemical mapping of tire and road wear particles for single particle analysis. *Sci. Total Environ.* 757 <https://doi.org/10.1016/j.scitotenv.2020.144085>.
- Kreider, M.L., Panko, J.M., McAtee, B.L., Sweet, L.L., Finley, B.L., 2010. Physical and chemical characterization of tire-related particles: comparison of particles generated using different methodologies. *Sci. Total Environ.* 408, 652–659. <https://doi.org/10.1016/j.scitotenv.2009.10.016>.
- Lange, K., Magnusson, K., Viklander, M., Blecken, G.-T., 2021. Removal of rubber, bitumen and other microplastic particles from stormwater by a gross pollutant trap - bioretention treatment train. *Water Res.* 202, 117457 <https://doi.org/10.1016/j.watres.2021.117457>.
- Lange, K., Österlund, H., Viklander, M., Blecken, G.-T., 2022. Occurrence and concentration of 20–100 µm sized microplastic in highway runoff and its removal in a gross pollutant trap – bioretention and sand filter stormwater treatment train. *Sci. Total Environ.* 809, 151151 <https://doi.org/10.1016/j.scitotenv.2021.151151>.
- Magnusson, K., Eliasson, K., Fråne, A., Haikonen, K., Hulten, J., Olshammer, M., Stadmark, J., Voisin, A., Miljöinstitutet, IVL Svenska, 2016. Swedish Source and Pathways for Microplastics to the Marine Environment - A Review of Existing Data, Number C 183. IVL Swedish Environmental Research Institute.
- Markiewicz, A., Strömvall, A.M., Björklund, K., Eriksson, E., 2019. Generation of nano- and micro-sized organic pollutant emissions in simulated road runoff. *Environ. Int.* 133, 105140 <https://doi.org/10.1016/j.envint.2019.105140>.
- Mattonai, M., Nacci, T., Modugno, F., 2022. Analytical strategies for the quantification of tire and road wear particles – a critical review. *Trends Anal. Chem.* <https://doi.org/10.1016/j.trac.2022.116650>.
- Mengistu, D., Heistad, A., Coutris, C., 2021. Tire wear particles concentrations in gully pot sediments. *Sci. Total Environ.* 769, 144785 <https://doi.org/10.1016/j.scitotenv.2020.144785>.
- Mitchell, C.J., Jayakaran, A.D., Jayakaran, A.D., 2023. Mitigating tire wear particles and tire additive chemicals in stormwater with permeable pavements. <https://doi.org/10.1016/j.scitotenv.2023.168236>.
- Monira, S., Bhuiyan, M.A., Haque, N., Shah, K., Roychand, R., Hai, F.L., Pramanik, B.K., 2021. Understanding the fate and control of road dust-associated microplastics in stormwater. *Process Saf. Environ. Protect.* 152, 47–57. <https://doi.org/10.1016/j.psep.2021.05.033>.
- Rasmussen, L.A., Lykkemark, J., Raaschou Andersen, T., Vollertsen, J., 2023. Permeable pavements: a possible sink for tyre wear particles and other microplastics? *Sci. Total Environ.* 869 <https://doi.org/10.1016/j.scitotenv.2023.161770>.
- Ruert, C., Rørdland, E.S., Okoffo, E.D., Reid, M.J., Meland, S., Thomas, K.V., 2021. Challenges with quantifying tire road wear particles: recognizing the need for further refinement of the ISO technical specification. *Environ. Sci. Technol. Lett.* <https://doi.org/10.1021/acs.estlett.0c00949>.
- Ruert, C., Vardy, S., Daniell, B., Charlton, N., Thomas, K.V., 2022. Tyre additive chemicals, tyre road wear particles and high production polymers in surface water at 5 urban centres in Queensland, Australia. *Sci. Total Environ.* 852 <https://doi.org/10.1016/j.scitotenv.2022.158468>.
- Rørdland, E.S., Gustafsson, M., Jaramillo-Vogel, D., Järnskog, I., Müller, K., Ruert, C., Rausch, J., Wagner, S., 2023a. Analytical challenges and possibilities for the quantification of tire-road wear particles. *TrAC, Trends Anal. Chem.* 165, 117121 <https://doi.org/10.1016/j.trac.2023.117121>.
- Rørdland, E.S., Heier, L.S., Lind, O.C., Meland, S., 2023b. High levels of tire wear particles in soils along low traffic roads. *Science of the Total Environment* 903. <https://doi.org/10.1016/j.scitotenv.2023.166470>.
- Rørdland, E.S., Lind, O.C., Reid, M., Heier, L.S., Skogsberg, E., Snilsberg, B., Gryteselv, D., Meland, S., 2022a. Characterization of tire and road wear microplastic particle contamination in a road tunnel: from surface to release. *J. Hazard Mater.* 435, 129032 <https://doi.org/10.1016/j.jhazmat.2022.129032>.
- Rørdland, E.S., Samanipour, S., Ruert, C., Okoffo, E.D., Reid, M.J., Heier, L.S., Lind, O.C., Thomas, K.V., Meland, S., 2022b. A novel method for the quantification of tire and polymer-modified bitumen particles in environmental samples by pyrolysis gas chromatography mass spectroscopy. *J. Hazard Mater.* 423 (Part A), 127092 <https://doi.org/10.1016/j.jhazmat.2021.127092>.
- Sutton, R., Franz, A., Gilbreath, A., Lin, D., Miller, L., Sedlak, M., Wong, A., Box, C., Holleman, R., Munno, K., Zhu, X., Rochman, C., 2019. Understanding Microplastic Levels, Pathways, and Transport, vol. 950. SFEI-ASC Publication, pp. 1–402.
- Swedish Land Survey, 2024. Minkarta lantmateriet [WWW Document]. URL <http://minkarta.lantmateriet.se/>, 4.4.24.
- Swedish Transport Administration, 2024. NVDB on web [WWW Document]. URL <http://nvdb2012.trafikverket.se/SeTransportnatverket>, 4.5.24.
- Tian, Z., Zhao, H., Peter, K.T., Gonzalez, M., Wetzel, J., Wu, C., Hu, X., Prat, J., Mudrock, E., Hettinger, R., Cortina, A.E., Biswas, R.G., Kock, F.V.C., Soong, R., Jenne, A., Du, B., Hou, F., He, H., Lundeen, R., Gilbreath, A., Sutton, R., Scholz, N.L., Davis, J.W., Dodd, M.C., Simpson, A., McIntyre, J.K., Kolodziej, E.P., 2021. A ubiquitous tire rubber-derived chemical induces acute mortality in coho salmon. *Science* 371, 185–189. <https://doi.org/10.1126/science.abd6951>, 1979.
- Unice, K.M., Kreider, M.L., Panko, J.M., 2013. Comparison of tire and road wear particle concentrations in sediment for watersheds in France, Japan, and the United States by quantitative pyrolysis GC/MS analysis. *Environ. Sci. Technol.* 47, 8138–8147. <https://doi.org/10.1021/es400871j>.

- Unice, K.M., Kreider, M.L., Panko, J.M., 2012. Use of a deuterated internal standard with pyrolysis-GC/MS dimeric marker analysis to quantify tire tread particles in the environment. *Int. J. Environ. Res. Publ. Health* 9, 4033–4055. <https://doi.org/10.3390/ijerph9114033>.
- Vijayan, A., Österlund, H., Magnusson, K., Marsalek, J., Viklander, M., 2022. Microplastics (MPs) in urban roadside snowbanks: quantities, size fractions and dynamics of release. *Sci. Total Environ.* 851, 158306 <https://doi.org/10.1016/j.scitotenv.2022.158306>.
- Vogelsang, C., Lusher, A.L., Dadkhah, M.E., Sundvor, I., Umar, M., Ranneklev, S.B., Eidsvoll, D., Meland, S., 2019. Microplastics in Road Dust – Characteristics, Pathways and Measures.
- Wagner, S., Hüffer, T., Klöckner, P., Wehrhahn, M., Hofmann, T., Reemtsma, T., 2018. Tire wear particles in the aquatic environment - a review on generation, analysis, occurrence, fate and effects. *Water Res.* 139, 83–100. <https://doi.org/10.1016/j.watres.2018.03.051>.
- Water Information System Sweden, 2024. Lillån [WWW Document]. URL. <https://viss.lansstyrelsen.se/Waters.aspx?waterMSCD=WA49319905>. (Accessed 10 April 2021).
- Wik, A., Dave, G., 2009. Occurrence and effects of tire wear particles in the environment - a critical review and an initial risk assessment. *Environ. Pollut.* 157, 1–11. <https://doi.org/10.1016/j.envpol.2008.09.028>.
- Winston, R.J., Witter, J.D., Tirpak, R.A., 2023. Measuring sediment loads and particle size distribution in road runoff: implications for sediment removal by stormwater control measures. *Sci. Total Environ.* 902, 166071 <https://doi.org/10.1016/j.scitotenv.2023.166071>.